In vitro bioactivity and antibacterial capacity of 45S5 Bioglass®-based compositions containing alumina and strontium

Article *in* Journal of Materials Research and Technology · July 2021

DOI: 10.1016/j.jmrt.2021.04.053

5 authors, including:

Mariana Silva de Araujo
Instituto de Pesquisas Energéticas e Nucleares
4 PUBLICATIONS **11** CITATIONS
SEE PROFILE

Belén Cabal
Spanish National Research Council
48 PUBLICATIONS **869** CITATIONS
SEE PROFILE

Jose F Bartolomé
Spanish National Research Council
117 PUBLICATIONS **2,592** CITATIONS
SEE PROFILE

S. R. H. Mello-Castanho
Instituto de Pesquisas Energéticas e Nucleares
75 PUBLICATIONS **546** CITATIONS
SEE PROFILE

Available online at www.sciencedirect.com

jmr&t Journal of Materials Research and Technology

journal homepage: www.elsevier.com/locate/jmrt

Original Article

In vitro bioactivity and antibacterial capacity of 45S5 Bioglass®-based compositions containing alumina and strontium

M.S. Araujo [a], A.C. Silva [a,1], B. Cabal [b], J.F. Bartolomé [c,*], S. Mello-Castanho [a]

[a] Nuclear and Energy Research Institute (IPEN), Center of Materials Science and Technology (CCTM), Laboratoy of Ceramic and Waste Processing (LaPCeRe), São Paulo/SP, 05508-000, Brazil

[b] Nanomaterials and Nanotechnology Research Centre (CINN), Consejo Superior de Investigaciones Científicas (CSIC), Universidad de Oviedo (UO), Principado de Asturias (PA), Avenida de la Vega 4-6, El Entrego, Asturias, 33940, Spain

[c] Instituto de Ciencia de Materiales de Madrid (ICMM), Consejo Superior de Investigaciones Científicas (CSIC), Madrid, 28049, Spain

ARTICLE INFO

Article history:
Received 19 January 2021
Accepted 19 April 2021
Available online 26 April 2021

Keywords:
Bioactive glasses
Alumina
Bioactivity
Antibacterial activity
Cytotoxicity

ABSTRACT

A modified 45S5 Bioglass® containing 2 mol% alumina and 2 mol% strontium oxide was prepared. In vitro bioactivity in powder and monolithic samples was conducted. Fourier transform infrared analysis and pH change in simulated body fluid were investigated for powder samples after 480 min of immersion. Additionally, X-ray diffraction and scanning electron microscopy after 7 and 14 days of immersion in simulated body fluid were investigated for monolithic samples. The formation of phosphate and carbonate phase precursors of hydroxycarbonate apatite was observed after 480 min for powder samples, and the hydroxycarbonate apatite pattern and morphology were confirmed after 7 days of immersion for monolithic samples. It seems that changes in composition did not affect reactivity but caused a decrease in the maxima of pH. Cytotoxicity and cell viability obtained by using the NCTC clone 929 cell line did not show any significant loss of cell viability or cytotoxicity. Moreover, after overnight incubation, the samples demonstrated safe disinfection for *Escherichia coli*. For these reasons, the use of these new bioactive glasses can be considered a promising alternative for the reconstruction of bone defects and even for the treatment and suppression of bone infections.

* Corresponding author.
E-mail address: jbartolo@icmm.csic.es (J.F. Bartolomé).

[1] In memoriam: Prof. Antonio Carlos da Silva passed away on 3 April 2021 from COVID-19 complications. AC was born on 5th May 1966. As a researcher and educator, he gave his time, energy and love to his students and research colleagues. His premature death is an immeasurable loss.

https://doi.org/10.1016/j.jmrt.2021.04.053

1. Introduction

45S5 Bioglass®, apart from being the first material to bond to bone, is still by far one of most widely investigated materials for its efficiency in the repair of damaged bone tissues [1]. However, cases that require implantation or bone grafting are of a vastly different nature, and thus, it has become clear that a single solution cannot efficiently attend to all medical cases encountered [2,3]. That is, each case is influenced by factors such as the patient's age and metabolism, severity and extent of the bone defect, and initial mechanical load [4,5].

Taking this into account, changes in 45S5 composition have been considered to achieve desired effects for intended applications. Indeed, the ability to modify and add elements in glass networks is helpful to tailor properties and adjust requirements [6–8]. The challenge is to achieve an optimum balance between biocompatibility and other physicochemical properties.

We have recently shown that the addition of low amounts of alumina and strontium in a 45S5 composition outperformed some well-known drawbacks of 45S5, such as a poor processing window and a high tendency to crystallize, apart from significantly enhancing mechanical and tribological properties [9,10].

Among various elements that could promote such adjustments, strontium is one of the elements well known for being a bone-seeking element and a common substitute for calcium in glass composition in addition to improving osteoblast activity and inhibiting osteoclast function, minimizing the fracture of bone [11,12]. Recent studies have indicated that small amounts of strontium (2.5 mol%) exhibit bacteriostatic behavior against *Staphylococcus aureus (S. aureus)* [13]. Inhibitory effects on *Escherichia coli (E. coli)* and *Porphyromonas gingivalis (P. gingivalis)* were also reported [14]. Aluminum has a significant effect on improving the mechanical properties of bioglass, despite affecting its material solubility and, consequently, its bioactivity [11,12]. However, in adequate quantities, the solubility can be adjusted to acceptable limits, allowing the hydroxyapatite layer to last for longer periods and still be capable of bonding to bone while increasing the mechanical properties [15].

The effect of both elements on bioactivity has not been investigated thus far, and slight differences can lead to completely different biological responses. Here, we focused on evaluating the effects of each ion (Sr and Al) to better understand their combined effect. We performed powder and monolithic in vitro bioactivity analysis followed by infrared spectroscopy and X-ray diffraction to show the changes in apatite formation of each sample. The aims of this study were to investigate the effect of this compositional modification of 45S5 Bioglass® on bioactivity and its antibacterial capacity against *E. coli*.

2. Materials and methods

2.1. Sample preparation

Table 1 lists the four bioactive glass compositions (mol%) studied in this work. A sample of Bioglass® 45S5 (BioH) was kept for comparative purposes. The glasses were prepared from reagent-grade (Vetec, Brazil) SiO_2 (99.0 wt%), CaO (99.0 wt %), Na_2CO_3 (95.0 wt%), Al_2O_3 (99.0 wt%), $Ca(H_2PO_4)\cdot 2H_2O$ (99.0%) and $Sr(NO_3)_2$ (99.0 wt%). Batches were obtained by melt quenching in a Pt–5%Au crucible at 1500 °C for 1 h in a vertical electric furnace. The glasses were cast into parallelepipedal bars ($10 \times 10 \times 10$ mm^3) molds, annealed at 500 °C for 2 h and slowly cooled to room temperature. The bars were then ground by ball milling to fine particulates and sieved to obtain particle sizes <50 μm.

Table 1 – Nominal glass composition (mol%).

Sample	SiO_2	P_2O_5	Na_2O	CaO	Al_2O_3	SrO
BioH (45S5)	46.1	2.6	24.4	26.9	–	–
BioAl	44.1	2.6	24.4	26.9	2.0	–
BioSr	45.2	2.5	23.9	26.4	–	2.0
BioAlSr	43.2	2.5	23.9	26.4	2.0	2.0

2.2. In vitro bioactivity analysis

The SBF solution was prepared following the Kokubo protocol [16]. After the solution was prepared, in vitro tests were performed on powder samples. The tests were conducted in a polyethylene container in which the powder samples with a particle size <50 μm were dispersed in SBF solution at a ratio of 75 mg of glass to 50 mL of solution. The tests were performed in triplicate, and the solutions were agitated at a rate of 60 rpm and maintained at 37 °C for 480 min (8 h). The pH of the SBF solution was verified using a digital pH meter (Oakton™, PC700) after immersion of samples for different periods (0, 5, 15, 30, 60, 120, 240 and 480 min). Then, after the total period of immersion (8 h), the powders were filtered through quantitative filter paper (3 μ, Nalgon), rinsed immediately with Milli-Q water and acetone to stop any further reaction and dried at 50 °C for 2 h. Fourier transform infrared spectrometry was performed by using a spectrometer (Bruker IFS 66 VS) with diffuse reflectance attachment within a range of 400–1600 cm^{-1} and a resolution of 2 cm^{-1}.

The same SBF solution was used for monolithic pieces. The samples were soaked in SBF in a water bath at 37 °C with agitation for up to 14 days. The ratio of the sample surface area to SBF solution volume was 0.1 cm^2 mL^{-1}, and the solution was replaced every two days. After immersion for 7 and 14 days, the samples were rinsed immediately with Milli-Q water and acetone to stop any further reaction and dried at 50 °C for 2 h. Posteriorly, the sample surfaces were characterized by X-ray diffraction (XRD) for phase identification by using a Bruker D8 ADVANCE diffractometer using CuKα radiation with 2θ from 10 to 70° and a step of 0.1°/s.

2.3. SEM-EDS

Scanning electron microscopy (SEM; TM2300, Hitachi High-Technologies Co., Tokyo, Japan) at an accelerating voltage of 15 kV was used to evaluate the surface morphology of the samples after the bioactivity study. The chemical composition of the surface was examined with an energy-dispersive X-ray spectrometer (EDS: EMAX-7000, Horiba Ltd., Kyoto, Japan) by using 9 kV-K that penetrates approximately 1 μm in depth.

2.4. Dynamic dissolution

Dissolution experiments were conducted based on the method adapted by Silva [17] employing a Soxhlet distillation column. Powders with a particle size <50 μm of each composition were encapsulated within a microtube containing filter paper and four slots. The samples were continually washed with distilled water in a cyclic distillation process at 90 °C. Periods of, 1, 3, 7 and 14 days were evaluated. At the end of each step, the powders were filtered, rinsed with acetone, dried at 50 °C for 2 h and weighed using an analytical precision balance (±0.00005 g).

2.5. Minimum inhibitory concentration (MIC) determination

A twofold broth dilution method was used for minimum inhibitory concentration (MIC) and minimum bactericidal concentration (MBC) determination. Twofold serial dilutions of the powder samples (concentration ranging from 1 mg mL^{-1} to 16 mg mL^{-1}) were prepared in tubes containing nutrient broth medium and an inoculum of *E. coli* (2.11×10^5 CFU mL^{-1}). A negative control containing only the cell inoculum in the growth medium was also prepared. After incubation for 24 h at 37 °C, bacterial growth was assessed by serial dilution plating. Nondirect determination of cell growth, such as culture turbidity, was used to determine the MIC. There is potential optical interference due to the light-scattering properties of the powdered glass. Consequently, the bacteriostatic effect of these samples was determined by performing a viable count after exposure of the bacteria to samples for a fixed time of 24 h.

2.6. Cytotoxicity assay

An in vitro test of cytotoxicity was performed using bulk samples according to ISO 10993-Part 5 by the neutral red uptake methodology employing the cell line NCTC clone 929 from American Type Culture Collection (ATCC) [18,19]. The test was conducted in triplicate, and for the positive and negative controls, a 0.02% phenol solution and alumina were used, respectively. The cytotoxicity potential of the samples is presented as a cytotoxicity index (IC50 (%)). This is the concentration of the extract that injures or kills 50% of the cell population in the assay due to toxic elements extracted from the sample. The complete assay was described by C. Santos et al. [20].

3. Results and discussion

3.1. In vitro bioactivity: powder samples

As already discussed in previous work [9,10], these samples are formed by an open silicate network interconnected mostly in a combination of Q^2_{Si} units, chains and rings. These associate with metastable materials, for which, in any liquid medium, the structure tends to seek and capture ionic species from the medium to constitute stable hydrated phases [21].

Carbonated hydroxyapatite formation is a prerequisite for glass bonds to bone/tissue. Its formation is a consequence of the dissolution process and generally follows the steps of usual alteration, that is, leaching, dissolution and precipitation [22]. The difference is that this process occurs at ~37 °C (body temperature), and the aqueous medium is the body fluid. After leaching, transition and precipitation of a silica-rich layer, a calcium-phosphate-rich layer is formed on top of it. This phase initially is amorphous and later crystallizes to a hydroxycarbonate apatite (HCA). When there are other ions present in glass, such as Sr^{2+} and Al^{3+}, the interaction between phosphate and the alkaline matrix can shift, resulting in related crystalline compounds. However, there is tolerance of the amount that can be substituted in the crystal lattice without compromising its structure [23,24].

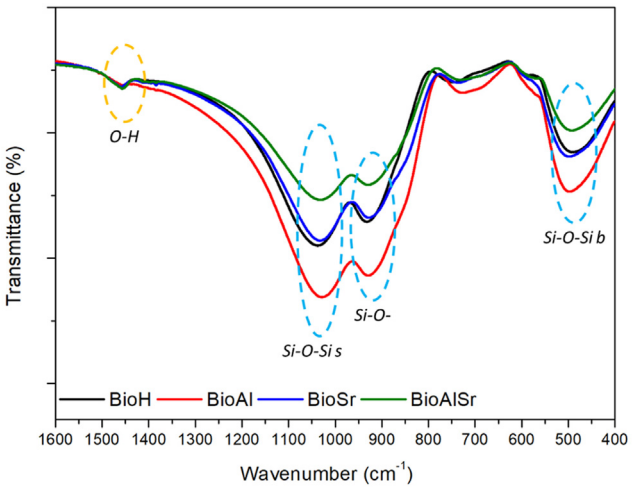

Fig. 1 – FT-IR of powder sample before SBF test.

The formation of HCA layers on glass particles was studied in simulated body fluid solution obtained according to the Kokubo protocol [16] and tested under Fredholm- [25] adapted conditions for high bioactive powder samples as described in section 2.2.

The formation of an HCA layer occurs while the silica characteristic bands decrease [26]. Fig. 1 presents the FTIR spectra of

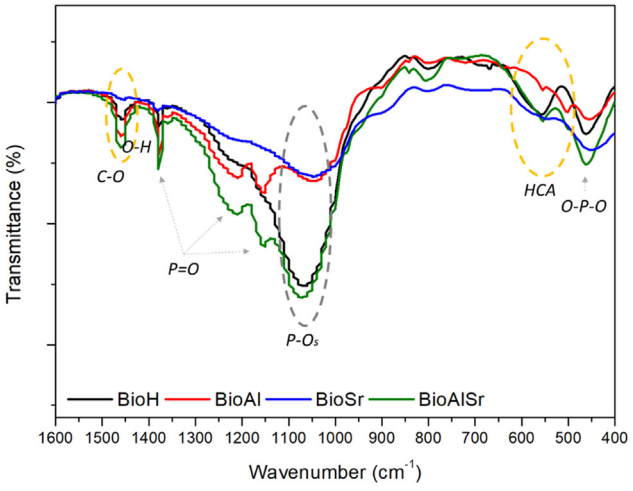

Fig. 2 – FT-IR of powder sample after SBF test (8 h).

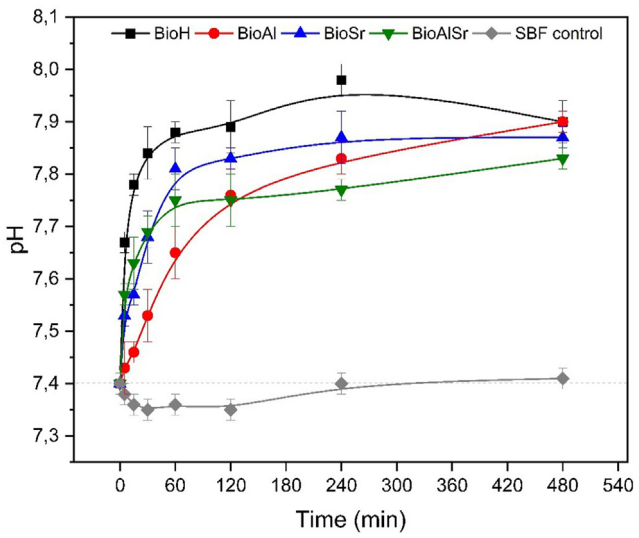

Fig. 3 – pH measurements during SBF test.

the powder glass samples as obtained. The spectra of samples before immersion exhibited a usual disordered feature, indicating a band at 940 cm^{-1} assigned to the structure Q^2_{Si} (Si–O (2NBO) and bands at ~ 1030 cm^{-1} and at 490 cm^{-1} associated with stretching and bending of $Q_{Si}{}^3$ units (Si–O–Si), respectively.

Fig. 2 shows the FTIR spectra after immersion in SBF. Time favored the appearance of phosphate and carbonate phases needed for HCA formation with prolonged exposition. A soaking time of 480 min was sufficient for reconfiguration of the existing features, and it can be observed that the bands at 1030, 940 and 490 cm^{-1} were substituted by a strong band at ~1060 cm^{-1} assigned to the P–O stretching vibration. This substitution is more evident for BioH and BioAlSr samples. Bands associated with amorphous and crystalline phosphorous can be identified all over the spectra at 460, 1150, 1210 and 1390 cm^{-1}. Additionally, minor peaks associated with HCA development can be observed at 1460 cm^{-1} for C–O stretching and 550 cm^{-1} for the crystalline phase of HCA.

In addition to FTIR, the medium was monitored by measuring the pH at 0, 5, 15, 30, 60, 120, 240 and 480 min. Fig. 3 shows the variation in pH of the SBF solution with each sample and the control solution as a function of time. As the sample powders have particle sizes in the same range, and the amount used was fixed, the variation in pH can be correlated to the composition of the glasses. The changes in pH relate to ion exchange and may vary with composition. Exchange is necessary to constitute a stable phase such as HCA. According to Jha and Singh, maximum degradation corresponds to the maximum pH change [27]. By considering this proposition, we can assume that BioAl and BioAlSr require more time to interact with the medium to reach maximum degradation, unlike samples BioH and BioSr. This might be due to the content of alumina in both samples since it is known that this compound affects glass dissolution. We can also observe that these samples (BioAl and BioAlSr) exhibit a decrease in the maxima of pH, related to the initial stage of dissolution, which comprises the cation exchange of ions such as Na^+, showing the influence of alumina in the dissolution process. As dissolution occurs, the greater the cation exchange is, the greater the pH until it reaches the maximum degradation mentioned above. This has already been observed in other samples containing alumina studied by Tripathi et al. [11,28,29].

Although the addition of alumina delayed the initial pH increase in BioAl, which is common in bioactive glasses with such a composition, its association with SrO reversed this effect. We can observe that BioAlSr, despite undergoing a decrease in maxima, had its initial rapid increase in pH restored [23,25]. We cannot presume that those pH maxima of samples BioAl and BioAlSr occurred at 480 min, when evaluation of dissolution mechanisms of all compositions was conducted, but we can consider that the results presented here supplement a recurrent drawback of bioactive glasses, which is a fast dissolution rate without losing reactivity. Investigation of alumina substitution of CaO content has shown that it reduces the reactivity and calcium phosphate formation [21]. On the other hand, its substitution to the detriment of P_2O_5 in phosphate-based glasses tends to provide an apatite layer that is more stable over a long period [15]. This

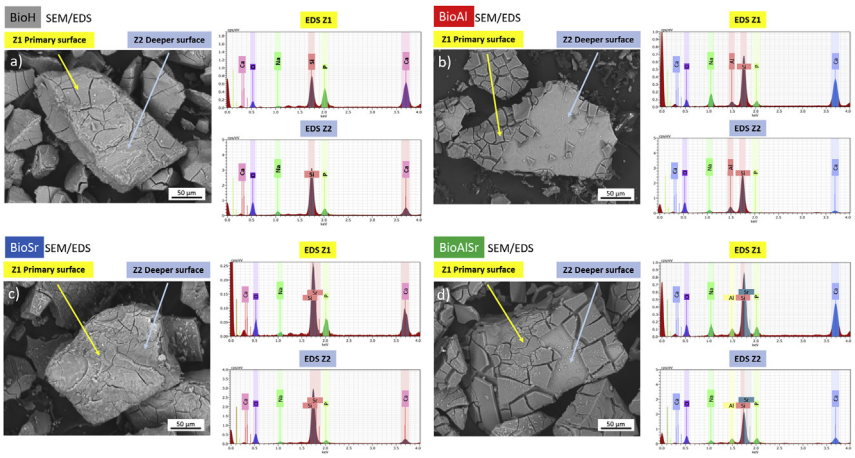

Fig. 4 – SEM/EDS micrographs of powder samples after the 8 h SBF test for a) BioH; b) BioAl; c) BioSr; d) BioAlSr.

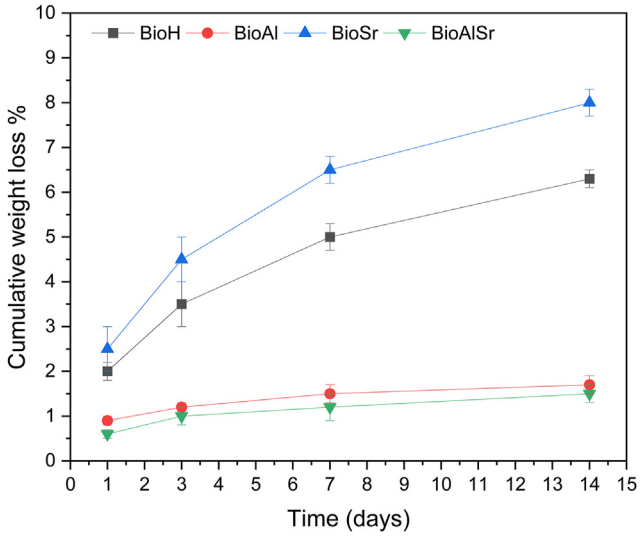

Fig. 5 – Cumulative weight loss (%) as a function of time (days) during the dissolution test.

is only possible because alumina is in the glass network as a former oxide, as in the BioAl and BioAlSr samples.

Fig. 4 shows the surface morphology and EDS spectra for samples after 480 min of immersion in SBF. As expected, the overall micrographs did not suggest any morphological characteristic formation of hydroxyapatite due to the short period of exposure. However, as degradation undoubtedly occurs, two surface patterns can be observed: one layer that is external and rich in calcium and phosphorous is identified as the primary surface in the images and the other layer that is more profoundly rich in silanol groups is identified as a deeper surface. Additionally, the EDS analysis confirms the differences in the composition of the layers.

Fig. 5 shows the cumulative weight loss as a function of time obtained after the dissolution test. For all the glass samples, a rising weight loss was observed as a function of time. However, BioAl and BioAlSr presented significantly lower losses than BioH and BioSr. The dissolution of alumina-containing samples appears to be slower and less intense, reaching a loss of only ~2% after 14 days. BioH and BioSr, in contrast, showed expressive and constant weight loss over time, reaching losses of 6% and 8%, respectively, after 14 days.

Considering the micrographs and dissolution rates, it appears that the samples with the slowest degradation had detached and peeled surfaces. In contrast, BioH and BioSr presented deeper surfaces that were less apparent, and greater amounts of Ca and P were found, probably because the greater the degradation was, the greater the reactivity. Nevertheless, detailed investigations of degradation and dissolution must be conducted.

3.2. *In vitro bioactivity: monolithic samples*

The formation of HCA layers on glass was studied in simulated body fluid according to the Kokubo protocol [16]. The XRD patterns of the glasses after 7 and 14 days of the bioactivity test are plotted in Fig. 6 a and b, respectively, as well as the representative diffractogram patterns of crystalline apatite (red lines in the graph). After 7 days, the HCA appearance is clear, with intense peaks in 2θ between 25 and 26° and between 31 and 33° associated with lattice planes of HA [30,31]. Minor peaks near 47, 49 and 53° have been observed and are also related to HA. After 14 days, the peaks in 2θ between 25 and 26° and between 31 and 33° increased their diffraction intensities, and slight narrowing can be noticed. In both periods, a slight displacement towards higher 2θ values was observed for samples containing strontium (BioSr and BioAlSr), instead of lower values, as observed by Srirangananthan et al. [23].

Figs. 7 and 8 show the surface morphology of all samples after 7 and 14 days of immersion in SBF. After 7 days of immersion, excluding BioAl (Fig. 7b), it is possible to observe the local formation of some globular deposits. Aggregate formation on top of BioH and BioAlSr with typical morphology of HCA can possibly indicate higher bioactivity of these samples. After 14 days, globular deposits were observed at the BioAl surface, suggesting that alumina addition did not inhibit HCA formation. BioH, BioSr and BioAlSr samples presented similar surfaces at 7 days with more aggregates.

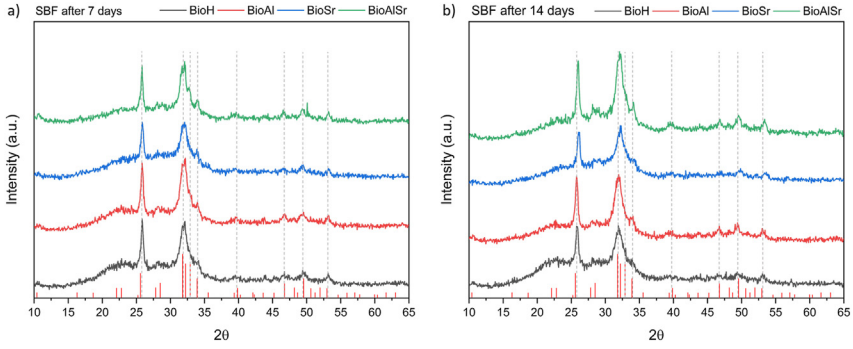

Fig. 6 – X-ray diffraction patterns of each monolithic sample after the SBF test at a) 7 days and b) 14 days. A generic diffractogram representative of well-crystalline hydroxyapatite (International Centre for Diffraction Data: data-set 00-09-0432) is also shown (red sticks).

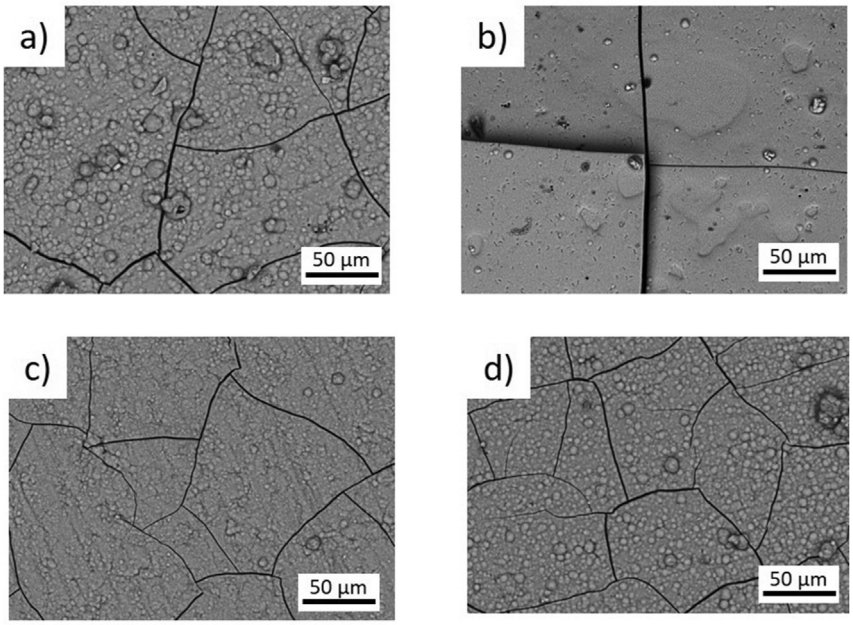

Fig. 7 – SEM micrographs after the SBF test at 7 days for a) BioH; b) BioAl; c) BioSr; d) BioAlSr.

3.3. *Antibacterial sensitivity to* E. coli

Sensitivity tests to *E. coli* bacteria were performed and are presented in Fig. 9. The results showed a logarithmic reduction in the number of colonies of *E. coli* after 24 h as a function of the concentration in ppm of the powder in the solution. The gray line in the graph represents the initial concentration of *E. coli* (~2,11 × 10^5 CFU mL^{-1}) for the different concentrations of powder. From the results, it can be observed that for all samples, a powder concentration above 4 ppm is required to achieve a logarithmic reduction higher than 7, indicating safe disinfection. BioH and BioSr presented a minimum inhibitory concentration (MIC) between 2 and 4 ppm, and BioAl and BioAlSr presented a minimum inhibitory concentration between 4 and 8 ppm. That is, after 24 h, the two samples containing alumina needed higher concentrations to inhibit the visible growth of a microorganism. Nevertheless, the minimum bactericidal concentration (MBC) was found to be 4 ppm for BioH and BioSr and 8 ppm for BioAl and BioAlSr. This behavior is directly connected to the rate of degradation of the samples since, as observed by Drago et al. [4,32], the increase in pH due to alkaline ion release makes the surrounding

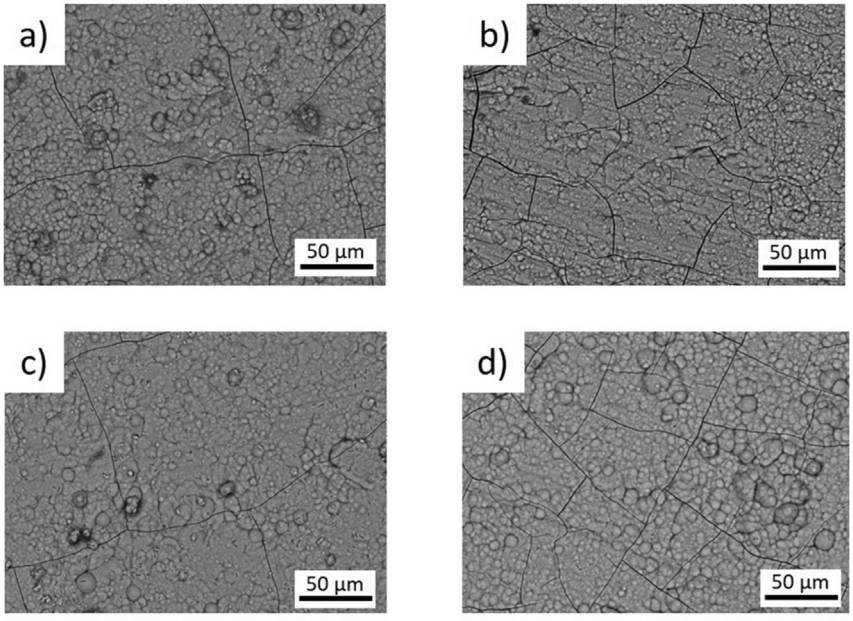

Fig. 8 – SEM micrographs after the SBF test at 14 days for a) BioH; b) BioAl; c) BioSr; d) BioAlSr.

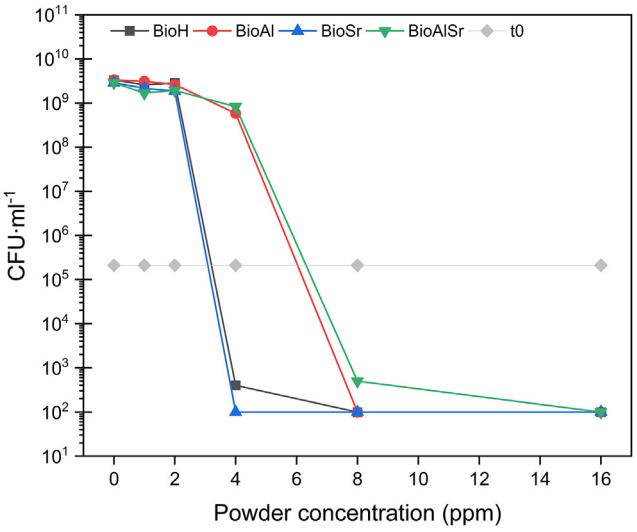

Fig. 9 – Colony forming units (CFU mL^{-1}) of *E. coli* versus concentration (ppm) of powder samples.

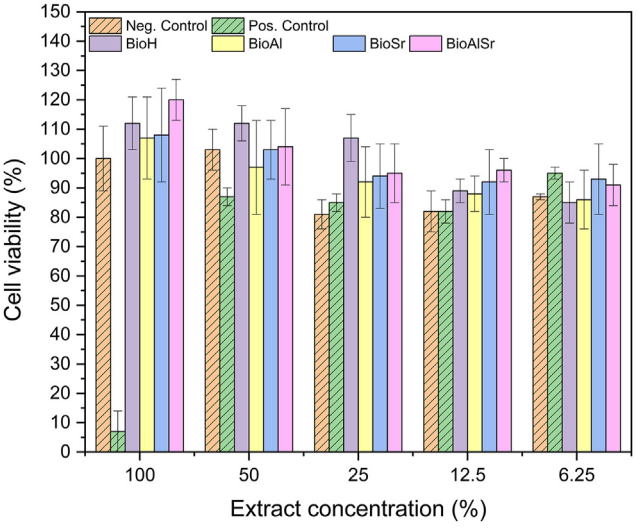

Fig. 10 – Cell viability (%) of BioH, BioAl, BioSr, BioAlSr and positive and negative controls.

environment inopportune for bacterial growth. Therefore, it can be presumed that higher rates will provide the environment needed to inhibit bacterial growth faster.

3.4. Cytotoxicity

It can be seen in Fig. 10 from the results that only the positive control showed cytotoxicity with an extract concentration of 100%; thus, all extracts from the 4 compositions of the glasses produced do not present cytotoxic potential. The analysis shows the percentage of viability for different concentrations of extracts. According to ISO 10993–5, samples can be considered noncytotoxic when the cell viability, that is, the number of live cells after the test, is above 70% at an extract concentration of 100%. From the results, it can be observed that at all extract concentrations, the samples reached a cell viability greater than 70%. At a concentration of 100%, the cell viability was above 90% for all samples. Hence, the samples tested can be considered noncytotoxic.

Investigations of in vitro dissolution and cellular adhesion are being performed. Tests evaluating the release of Sr ions are also being conducted to verify the potential of controlled ion release therapies. The changes made in composition did not affect the reactivity of the glass, proving the efficiency of the strict design of the composition in view of the well-known influence of the composition–property relationship on these materials.

4. Conclusions

By adding 2 mol% Al_2O_3 and 2 mol% SrO to 45S5, the bioactivity was preserved even as the glass degradation decreased because of the alumina capability. The formation of phosphate and carbonate phase precursors of HCA was observed after 480 min for powder samples, and after 7 and 14 days, SEM analysis of monolithic samples confirmed HCA formation. XRD patterns confirmed that the substitutional ions adapted to the crystal lattice of HCA without compromising its structure. None of the samples evaluated were considered cytotoxic by the neutral red uptake methodology. Furthermore, after overnight incubation, the samples exhibited safe disinfection for *E. coli*. The results showed that the designed composition achieved the combined effect of antibacterial activity and biocompatibility, contributing to the field of bioactive glasses used for bone regeneration applications.

Declaration of Competing Interest

The authors declare that they have no known competing financial interests or personal relationships that could have appeared to influence the work reported in this paper.

Acknowledgments

This research was performed with support from the Brazilian government through the funding agencies CAPES (CsF/PDSE-Project No 88881.189953/2018–01), CNPq (GD-Project No 142172/2016–2, Universal Research Project No 481260/2012–9 and PD. 312135/2016–5) and FAPESP (Project No 1999/01924–2).

REFERENCES

[1] Baino F, Hamzehlou S, Kargozar S. Bioactive glasses: where are we and where are we going? J Funct Biomater 2018;9:25.

[2] Fiume E, Barberi J, Verné E, Baino F. Bioactive glasses: from parent 45S5 composition to scaffold-assisted tissue-healing therapies. J Funct Biomater 2018;9:24.
[3] Esteban-Tejeda L, Smirnov A, Prado C, Moya JS, Torrecillas R, Bartolomé JF. Multifunctional ceramic-metal biocomposites with Zinc containing antimicrobial glass coatings. Ceram Int 2016;42:7023–9.
[4] Drago L, Toscano M, Bottagisio M. Recent evidence on bioactive glass antimicrobial and antibiofilm activity: a mini-review. Materials 2018;11:326.
[5] Lopez-Esteban S, Bartolomé JF, Diaz LA, Esteban-Tejeda L, Prado C, Lopez-Piriz R, et al. Mechanical performance of a biocompatible biocide soda–lime glass-ceramic. J Mech Behav Biomed 2014;34:302–12.
[6] Martinez A, Guitián F, López-Píriz R, Bartolomé JF, Cabal B, Esteban-Tejeda L, et al. Bone loss at implant with titanium abutments coated by soda lime glass containing silver nanoparticles: a histological study in the dog. PloS One 2014;9:e86926.
[7] Lopez-Piriz R, Sola-Linares E, Granizo J-J, Diaz-Guemes I, Enciso S, Bartolomé JF, et al. Radiologic evaluation of bone loss at implants with biocide coated titanium abutments: a study in the dog. PloS One 2012;7:e52861.
[8] Cabal B, Cafin F, Esteban-Tejeda L, Alou L, Bartolomé JF, Sevillano D, et al. Inhibitory effect on in vitro Streptococcus oralis biofilm of a soda-lime glass containing silver nanoparticles coating on titanium alloy. PloS One 2012;7:e42393.
[9] Araujo MS, Bartolomé JF, Mello-Castanho S. Tribological and mechanical behaviour of 45S5 Bioglass®-based compositions containing alumina and strontium. Ceram Int 2020;46:24347–54.
[10] Araujo MS, Silva AC, Bartolomé JF, Mello-Castanho S. Structural and thermal behavior of 45S5 Bioglass®-based compositions containing alumina and strontium. J Am Ceram Soc 2020;103:3620–30.
[11] Tripathi H, Rath C, Kumar AS, Manna PP, Singh SP. Structural, physico-mechanical and in-vitro bioactivity studies on SiO_2–CaO–P_2O_5–SrO–Al_2O_3 bioactive glasses. Mater Sci Eng C 2019;94:279–90.
[12] Rabiee SM, Nazparvar N, Azizian M, Vashaee D, Tayebi L. Effect of ion substitution on properties of bioactive glasses: a review. Ceram Int 2015;41:7241–51.
[13] Li Y, Stone W, Schemitsch EH, Zalzal P, Papini M, Waldman SD, et al. Antibacterial and osteo-stimulatory effects of a borate-based glass series doped with strontium ions. J Biomater Appl 2016;31:674–83.
[14] Zhang J, Zhao S, Zhu Y, Huang Y, Zhu M, Tao C, et al. Three-dimensional printing of strontium-containing mesoporous bioactive glass scaffolds for bone regeneration. Acta Biomater 2014;10:2269–81.
[15] El-Kheshen AA, Khaliafa FA, Saad EA, Elwan RL. Effect of Al_2O_3 addition on bioactivity, thermal and mechanical properties of some bioactive glasses. Ceram Int 2008;34:1667–73.
[16] Kokubo T, Kushitani H, Sakka S, Kitsugi T, Yamamuro T. Solutions able to reproducein vivo surface-structure changes in bioactive glass-ceramic A-W3. J Biomed Mater Res 1990;24:721–34.
[17] Silva AC, Mello-Castanho SRH. Vitrified galvanic waste chemical stability. J Eur Ceram Soc 2007;27:565–70.
[18] Biological evaluation of medical devices – Part 5: tests for in vitro cytotoxicity. 2009.
[19] Rogero SO, Malmonge SM, Lugão AB, Ikeda TI, Miyamaru L, Cruz ÁS. Biocompatibility study of polymeric biomaterials. Artif Organs 2003;27:424–7.
[20] Santos C, Ribeiro S, Daguano JKMF, Rogero SO, Strecker K, Silva CRM. Development and cytotoxicity evaluation of SiAlONs ceramics. Mater Sci Eng C 2007;27:148–53.
[21] Hupa L, Fagerlund S, Massera J, Björkvik L. Dissolution behavior of the bioactive glass S53P4 when sodium is replaced by potassium, and calcium with magnesium or strontium. J Non-Cryst Solids 2016;432:41–6.
[22] Da Silva AC. Structure and percolation of bioglasses. In: Adv struct mater. Cham: Springer; 2016. p. 49–84.
[23] Sriranganathan D, Kanwal N, Hing KA, Hill RG. Strontium substituted bioactive glasses for tissue engineered scaffolds: the importance of octacalcium phosphate. J Mater Sci Mater Med 2016;27:39.
[24] Wetzel R, Brauer DS. Apatite formation of substituted Bioglass 45S5: SBF vs. Tris. Mater Lett 2019;257:126760.
[25] Fredholm YC, Karpukhina N, Brauer DS, Jones JR, V Law R, Hill RG. Influence of strontium for calcium substitution in bioactive glasses on degradation, ion release and apatite formation. J R Soc Interface 2012;9:880–9.
[26] Kontonasaki E, Zorba T, Papadopoulou L, Pavlidou E, Chatzistavrou X, Paraskevopoulos K, et al. Hydroxy carbonate apatite formation on particulate bioglass in vitro as a function of time. Cryst Res Technol 2002;37:1165–71.
[27] Jha P, Singh K. Effect of MgO on bioactivity, hardness, structural and optical properties of SiO2–K2O–CaO–MgO glasses. Ceram Int 2016;42:436–44.
[28] Tripathi H, Kumar Hira S, Sampath Kumar A, Gupta U, Pratim Manna P, Singh SP. Structural characterization and in vitro bioactivity assessment of SiO_2–CaO–P_2O_5–K_2O–Al_2O_3 glass as bioactive ceramic material. Ceram Int 2015;41:11756–69.
[29] Arepalli SK, Tripathi H, Hira SK, Manna PP, Pyare R, Singh SP. Enhanced bioactivity, biocompatibility and mechanical behavior of strontium substituted bioactive glasses. Mater Sci Eng C 2016;69:108–16.
[30] Yu Y, Bacsik Z, Edén M. Contrasting in vitro apatite growth from bioactive glass surfaces with that of spontaneous precipitation. Materials 2018;11:1690.
[31] Calasans-Maia Mônica Diuana, Melo Bruno Raposo de, Alves Adriana Terezinha Neves Novellino, Resende Rodrigo Figueiredo de Brito, Louro Rafael Seabra, Sartoretto Suelen Cristina, et al. Cytocompatibility and biocompatibility of nanostructured carbonated hydroxyapatite spheres for bone repair. J Appl Oral Sci 2015;23:599–608.
[32] Drago L, De Vecchi E, Bortolin M, Toscano M, Mattina R, Romanò CL. Antimicrobial activity and resistance selection of different bioglass S53P4 formulations against multidrug resistant strains. Future Microbiol 2015;10:1293–9.